PORT SAID ENGINEERING RESEARCH JOURNAL
Faculty of Engineering - Port Said University
Volume 22 No. 1 March 2018 pp. 127:139

Numerical Investigation on Fluid Flow and Heat Transfer Characteristics for High Viscous Fluids inside Axially Rotating Tubes

Eng. Riam Nagi Bin Break[1], Dr. A.M. Saif [2], Dr. M.M. Shatat[3], Prof. Dr. A.M.I. Mohamed[4] and **Prof. Dr. N. N. Mikhael[5]**

ABSTRACT

This study presents the numerical investigation of the fluid flow and heat transfer characteristics for three different high viscous fluids (Engine oil, Oil (SN-500) and Ethylene glycol) flowing inside horizontal rotating tubes. A computational fluid dynamics (CFD) methodology using ANSYS FLUENT 14.0 is used to perform the numerical analysis by solving the Navier-Stokes and energy equations through the viscous model at all cases of rotation Reynolds numbers and Reynolds numbers. The investigation is conducted at rotation speed of 25, 50, 100, 500, 1000 and 2000 rpm and Reynolds number ranged between 5 and 10 for Engine oil, 54 and 109 for Oil (SN-500) and 425 and 849 for Ethylene glycol. The results revealed that, enhancement of heat transfer in the tubes with Ethylene glycol (lower viscous fluid) increases slightly with the further increase in rotation speed. This is because of the viscous effects which are observed significantly larger in the tubes with Ethylene glycol than those in the tubes with Engine oil and Oil (SN-500). These effects weakened growing of the tangential velocity component in the flow. In the tubes with Engine oil and Oil (SN-500), the maximum values of thermal performance factor are found at rotation speed of 1000 rpm, whereas, in the tubes with Ethylene glycol are occurred at rotation speed of 100 rpm. The value of the maximum thermal performance is about 2.1 for tube with Engine oil at a Reynolds number of 10, 1.6 for tube with Oil (SN-500) at a Reynolds number of 109 and 1.44 for tube with Ethylene glycol at a Reynolds number of 849.

KEYWORDS: Rotating tubes, fluid flow, heat transfer, high viscous fluids, CFD.

1. INTRODUCTION

Laminar flow in the rotating tubes is becoming interesting subject over the years, due to its practical importance in wide variety of engineering situations, especially in the rotating heat exchangers, which work with high viscous liquids, used in some chemical process and food industry.

The influence of tube rotation on the flow is depending on whether the flow is laminar or turbulent. In the laminar flow rotation has a destabilizing effect, due to the increase in the fluid velocity at the surface of the rotating tube. Turbulent flow on the other hand, is stabilized by rotation, because of the strong relaminarization caused by the centrifugal forces, which become predominant with the increase in rotation speed. Many theoretical and experimental studies had been conducted to study the flow and heat transfer characteristics inside rotating tubes, White [1] conducted experiment to measure the pressure loss in hydro-dynamically fully developed region of an axially rotating tube at rotation speed, n= 250, 500, 1000, 1500, 2000, 2560 and 3120 rpm. In this experiment the water was used as a testing fluid with Reynolds number, $Re \leq 10000$. It has been shown that the rotation considerably reduces the pressure loss in the turbulent flow regime, but at values of Re corresponding to laminar flow in a stationary tube the pressure loss is increased. Pedly [2] studied effect of pipe rotation on the velocity profiles in hydrodynamic entrance region at very low Re. The study revealed that, there is critical Re of 82.9 above which the laminar flow in the rotating pipe becomes unstable. These results have been experimentally confirmed by Najib et al. [3]. Instability of the laminar boundary layer developing in the inlet region of an axially rotating pipe has been studied experimentally by Nishibori et al. [4]. The experimental range of the Re and rotation rate was $4\times10^4 \leq Re \leq 9\times10^4$ and $0 \leq N \leq 1.4$, respectively. Air was used as a testing fluid. Results showed that, the increase in the rotation speed of the pipe increases occurrence of the spiral vortices inside the laminar boundary layer which cause upstream shift of the transition point from laminar to turbulent flow. Whereas, when the rotation speed is comparatively small, the spiral vortices, which have been produced in the entrance region, die away in the downstream sections due to the stabilizing effect of the rotation. The effects of tube rotation on the velocity and temperature distribution, on the friction coefficient and on the heat transfer in laminar and turbulent flow for fluids flowing inside tubes with rotation Reynolds number (Re_ω) ranging between 500-4000 and Re (Re) between 500-10^4, were examined experimentally by Reich

[1] Mechanical Power Department
[2, 3, 4, 5] Mechanical Power Department
Faculty of Engineering
Port Said University

and Beer [5, 6]. Their results showed that, the tube rotation causes a destabilization of the laminar flow, which becomes turbulent due to rotation. The results also showed that, the rotation has a very marked influence on the suppression of the turbulent motion, because of the strong relaminarization caused by the centrifugal forces which becomes predominant with the increase in rotation speed. Imao et al. [7] studied numerically the velocity profiles of the laminar flow in the developing region of an axially rotating pipe and compared the numerical results with experimental results obtained when a uniform axial flow is introduced. It was found that, the axial velocity in the rotating pipe exceeds the value of the Poiseuille flow at the center, and the backward flow appears near the pipe wall as the rotation rate becomes large. Experiments also showed that the flow is destabilized at rotation rate, N = 3 and the development of the flow is delayed. Soong et al. [8] studied experimentally the convective heat transfer in radially rotating isothermal rectangular ducts with different aspect ratios. In this study, the rotation speed up to 3000 rpm was used. The main flow Re was ranged from 700 to 20,000. They concluded that, the convective heat transfer is affected by secondary flows resulting from Coriolis force and growth and strength of the secondary flow depend on the rotation speed. The aspect ratio of the duct may affect the secondary flow and, therefore, it is also a critical parameter in the heat transfer mechanism. Weigand and Beer [9] studied numerically the interaction between turbulence suppression and tube rotation in the rotational entrance region of a pipe rotates about its axis. Re and rotation rate were 5000-20000 and 0-3, respectively. The results showed that, tube rotation will enhance the thermal entrance length, because of flow laminarization produced by centrifugal forces. Kuo and Wang [10] investigated experimentally the effects of rotation and aspect ratio on the convective heat transfer of air flows in rotating rectangular ducts with a uniform wall heat flux. Re and the rotation number (R_ω) were between 1000-15000 and 0-0.32, respectively. The cross sectional aspect ratio was 0.5, 1.0 and 2.0. The results showed that the higher the rotation number, the greater the enhancement of the heat transfer rate, especially at the pressure side. The largest heat transfer enhancement is seen for aspect ratio, AR = 1.0, and the enhancement for AR = 0.5 is greater than that for AR = 2. Cheng and Wang [11] studied experimentally the stabilizing (relaminarization) and destabilizing (early transition from laminar to turbulent flow) effects of Coriolis forces in the rotating radial straight pipes, with Re ranging between 500-4500 and rotation speed, n = 0-200 rpm,. In this study the air was used as a working fluid. The results showed that, Coriolis forces in the rotating radial straight pipes have both the destabilizing and stabilizing effects, leading to the early transition from laminar to turbulent flow at Re = 1500 and relaminarization process at Re = 4500, respectively.. Torii and Yang [12] investigated numerically the rotational effects on secondary flow phenomena in an axially rotating flow passage with sudden expansion or contraction. Water was used as the working fluid. The Re and the rotation rate ranged between 250-2000 and 0-2, respectively. It is disclosed from the study that: (1) when laminar flow introduces into an axially rotating pipe with expansion, the stretch of the secondary flow zone is amplified with an increase in the rotation rate and Re, and (2) in contrast, for axially rotating pipe flows with contraction, the secondary flow region is somewhat suppressed due to pipe rotation, and the change is slightly affected by the rotation rate and Re. Convective heat transfer in the rotating helical pipes with circular cross section was investigated theoretically by Chen et al. [13] to examine the combined effects of rotation (Coriolis force), and curvature (centrifugal force) on the heat transfer. It was assumed that the fluid flow is steady laminar, hydro-dynamically and thermally fully developed and the wall heat flux and the wall temperatures were both uniform. It was found that, the Nu ratio increases for co-rotation with force ratio F (the ratio of the Coriolis force to the centrifugal force) increases, but for counter-rotation, the Nu ratio decreases and reaches its minimum about 1 at F = -1. The evolution of Re on the laminar flow in an axially rotating pipe was investigated numerically by Ojo et al. [14] for rotation rates of N = 0, 2, 4 and 6 at different downstream sections, x = 0.1, 0.6 and 1.1. In this work water was used as a testing fluid with Re = 20, 30, 40, 50 and 60. The results showed that, when laminar flow is introduced into an axially rotating pipe, an adverse or large pressure gradient in the axial direction is generated and this causes a flow reversal to occur near the pipe wall at a section near the inlet. The flow approaches a forced vortex type due to large tangential and radial velocity experienced by the fluid and with an increase in Re.

Although a lot of the research works provide detailed information on the flow phenomena and heat transfer in the rotating tubes, but most of these works were confined on using fluids with low Prandtl numbers, such as air and water. Study of the flow and thermal fields due to rotation by using highly viscous fluids is very rare in the open literature. Therefore, the study using these fluids in rotating tubes is still required to fill the research gap. The aim of the present work is to study effect of rotation on the flow and thermal fields for the high viscous fluids inside rotating tubes.

2. PHYSICAL MODEL

A horizontal smooth steel tube with 1000 mm in length (L) and 20 mm in diameter (D) is used as testing section. The thickness of the tube is 1mm. Tube rotates about its axis at a constant angular velocity, ω. Wall temperature is assumed constant at 300˚C. Engine oil, Oil (SN-500) and Ethylene glycol are selected as working fluids with constant inlet temperature of 25˚C. The configuration and cylindrical coordinate system of the flow is shown in Fig. 1. Properties of fluids are listed in Table 1.

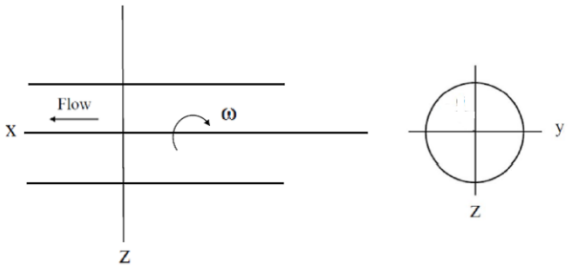

Top view Side view

Fig.1 The coordinates of the rotating tube.

3. MATHEMATICAL MODEL

The governing equations of the theoretical model consist of a set of fluid flow partial differential equations (Navier–Stokes equations, which represent continuity, momentum and the energy equations). The flow in the present study is considered to be three dimensional, laminar, steady and incompressible. No-slip boundary condition at the tube wall is implemented.

The basic model equations in inertial (non-accelerating) reference frame can be written as follows [15]:

Continuity equation:

$$\frac{\partial(\rho u_i)}{\partial x_i} = 0 \quad (1)$$

Momentum equation:

$$\frac{\partial}{\partial x_j}\left(\rho u_i u_j\right) = -\frac{\partial p}{\partial x_i} + \frac{\partial}{\partial x_j}\left[\mu\left(\frac{\partial u_i}{\partial x_j} + \frac{\partial u_j}{\partial x_i}\right)\right] \quad (2)$$

Energy equation:

$$\frac{\partial}{\partial x_j}\left(\rho u_j C_p T - k\frac{\partial T}{\partial x_j}\right) = 0 \quad (3)$$

The governing equations in moving reference frame (non-inertial reference frame) are augmented by additional acceleration terms that appear in the momentum equation due to the transformation from the stationary to the moving reference frame. However, the governing equations of fluid flow and heat transfer in steadily moving reference frame are as follows:

Continuity equation:

$$\nabla \cdot \rho\vec{v}_r = 0 \quad (4)$$

Momentum equation:

$$\nabla \cdot (\rho\vec{v}_r\vec{v}) + \rho\,[\vec{\omega} \times (\vec{v} - \vec{v}_t)] = -\nabla p + [\mu\,(\nabla\vec{v})] \quad (5)$$

Energy equation:

$$\nabla \cdot \left(\rho\vec{v}_r C_p T\right) = \nabla(k\,\nabla T) \quad (6)$$

Where

$$\vec{v}_r = \vec{v} - \vec{u}_r\,,\vec{u}_r = \vec{v}_t + \vec{\omega} \times \vec{r} \quad (7)$$

In the above equations, $\vec{v}_r$ is the relative velocity (the velocity viewed from the moving frame), $\vec{v}$ is the absolute velocity (the velocity viewed from the stationary frame), $\vec{u}_r$ is the velocity of the moving frame relative to the inertial reference frame, $\vec{v}_t$ is the translational frame velocity and $\vec{\omega}$ is the angular velocity. The term$(\vec{\omega} \times \vec{\omega} \times \vec{r})$ represents the Coriolis and centripetal accelerations.

The associated system boundary conditions of the governing equations are listed in Table 2.

The Re, Nu, friction factor (f) and thermal performance factor (TPF) proposed by Webb [16] are defined as follows:

$$Re = \frac{\rho u_i D}{\mu} = \frac{u_i D}{\nu} \quad (8)$$

$$Nu = \frac{hD}{k_f} \quad (9)$$

$$C_f = \frac{\tau_s}{\frac{\rho u_i^2}{2}} = \frac{f}{4} \quad (10)$$

$$TPF = \frac{(Nu_\omega/Nu_s)}{(f_\omega/f_s)} \quad (11)$$

Rotation Reynolds number is computed by equation 12

$$Re_\omega = \frac{\omega D^2}{\nu} \quad (12)$$

To calculate the average convective heat transfer coefficient inside the tube, the general governing heat balance equation is used as

$$\dot{Q} = hA_s\Delta T_m = \dot{m}C_p\,(T_e - T_i) \quad (13)$$

Where

$$\Delta T_m = \frac{T_i - T_e}{\ln\left[\frac{(T_s - T_e)}{(T_s - T_i)}\right]} \quad (14)$$

4. NUMERICAL METHOD

ANSYS FLUENT 14.0 is chosen as the CFD a tool for this work. FLUENT works on the finite volume method to solve the above governing equations accompanied with boundary conditions. The second order upwind discretization scheme for momentum and energy equations is employed in the numerical model. The pressure - velocity coupling is handled by the Coupled algorithm. In addition, convergence criteria of 10^{-3} for continuity and velocity components and 10^{-6} for energy are used.

Grid independent test has been performed for the physical model. The unstructured grid is used for meshing, as depicted in Fig. 2. The grid is highly concentrated near the tube wall. Four grid systems (mesh 1, mesh 2, mesh 3 and mesh 4) with about 301,408, 499,940, 1,249,578 and 1,505,957 elements are adopted to calculate grid independence, at constant Re and at the same boundary conditions. The comparison had been hold between the predicated values of the estimated pressure and fluid velocity at a specified point in the flow domain. The solution accuracy is measured by the value of the percentage difference between the flow variable of certain mesh and same flow variable of mesh 4. The result of the mesh independence test is shown in Fig. 3, which demonstrates that, the difference between the calculated results of 1,249,578 elements (mesh 3) and 1,505,957 elements (mesh 4) are very small. Therefore, the gird

system with 1,249,578 elements is adopted for the computational domain to give the acceptable accuracy of the solution, reasonable convergence of the solution, and best executing time.

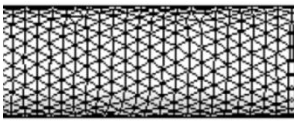

Fig.2 Part of the tube with unstructured grid generation.

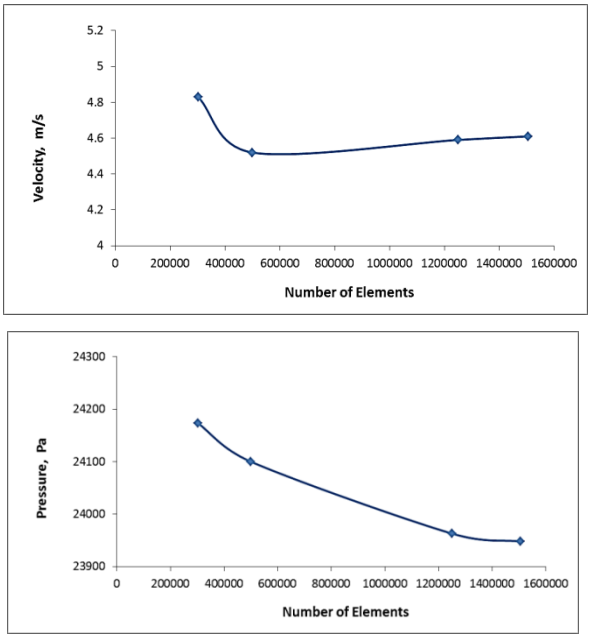

Fig.3 Grid independence test.

5. CFD SIMULATION MODEL VALIDATION

The accuracy of the numerical solution validated by comparing the experimental data of the friction factor ratio obtained by White [1] in the rotating plain tube with the predicted numerical results, using ANSYS Fluent 14.0. The comparison is conducted under similar operating conditions and water is used as working fluid. Rotation speed, n = 250 rpm and Re = 1700 and 1900 are used in this validation. The comparison between the predicted numerical results and the experimental results obtained by White [1] is shown in Fig.4. As seen in this figure, the deviation between the numerical results and the experimental results is limited and the maximum generated error is about 10%.

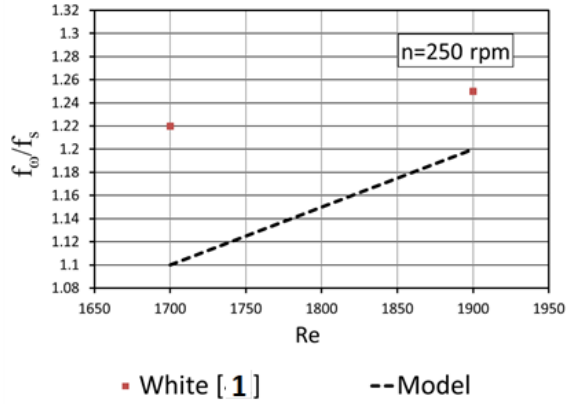

Fig.4 Comparison between numerical and experimental results of the friction factor ratio with Re, for water in the rotating plain tube.

6. RESULTS AND DISCUSSION

Different series of simulations under same operating condition are performed to investigate the effect of tube rotation on the fluid flow and heat transfer characteristics for high viscous fluids flowing inside tubes. Six tube rotation speeds of 25, 50, 100, 500, 1000 and 2000 rpm are used within the inlet velocities of 0.3, 0.4, 0.5 and 0.6 m/s. Table 3 lists the range of operating dimensionless parameters considered in the present work. Average Nu and total pressure drop along the rotating tubes are estimated and explained. The different results obtained from the simulations are compared with each other and the stationary tubes, too. Flow and thermal fields are investigated at u_i = 0.6 m/s and n = 1000 rpm.

6.1 FLOW FIELD INVESTIGATIONS

The dimensionless axial velocity profiles in stationary and rotating tubes are plotted from the entrance until locations in which the velocity profiles are developed which is equal to 0.011 m in the tubes with Engine oil, 0.11 m in the tubes with Oil (SN-500) and 0.85 m in the tubes with Ethylene glycol.

Effect of tube rotation on the axial velocity distribution is shown in Figs. 5 and 6(A, B and C). It can be seen that, in the tubes with Engine oil and Oil (SN-500), rotation increases the axial velocity profiles at the center than that for stationary tubes. This change in the velocity profiles is because of the increase in pressure loss when the tube is rotated. While in the tubes with Ethylene glycol, rotation considerably reduces the developing length, as a result of the flow deceleration. In general, rotation strongly influences the flow in the tube with Ethylene glycol due to its low viscosity that made it more affected by rotation than Engine oil and Oil (SN-500).

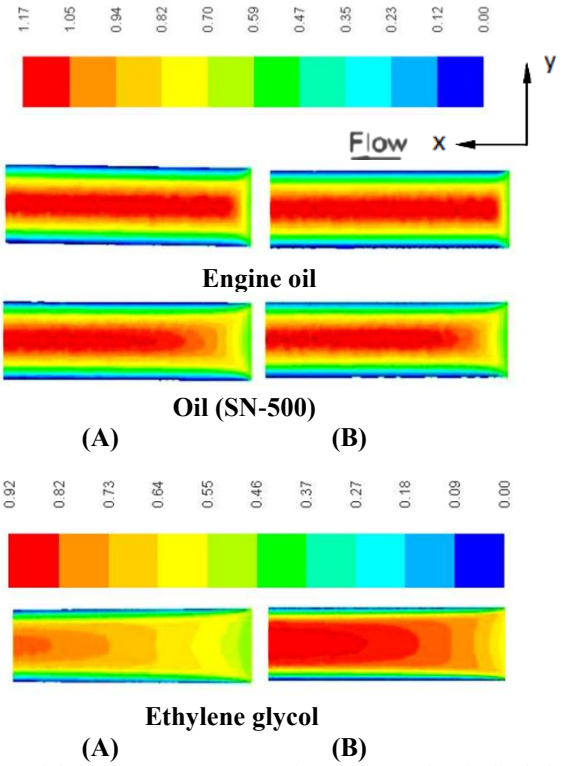

Fig.5 Axial velocity component (u, m/s) contours on longitudinal planes, from tube inlet to X* = 0.15, for all fluids in the stationary and rotating tubes, at u_i = 0.6 m/s, n = 1000 rpm. (A): Stationary tubes, (B): Rotating tubes.

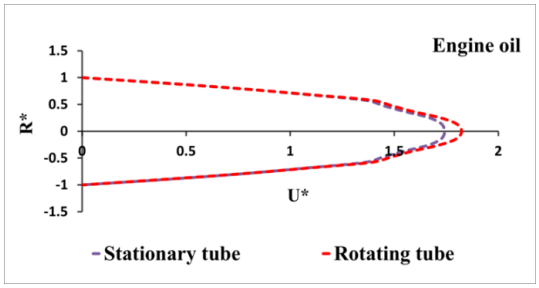

Fig.6(A) The predicted dimensionless axial velocity (U*) profiles on cross-sectional planes, at position, X* = 0.011 from tube inlet, for Engine oil in the stationary and rotating tubes, at u_i = 0.6 m/s, n = 1000 rpm.

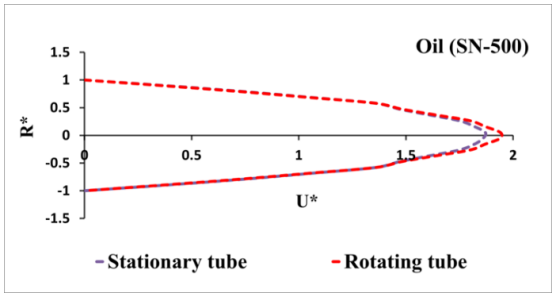

Fig.6(B) The predicted dimensionless axial velocity (U*) profiles on cross-sectional planes, at position, X* = 0.11 from tube inlet, for Oil (SN-500) in the stationary and rotating tubes, at u_i = 0.6 m/s, n = 1000 rpm..

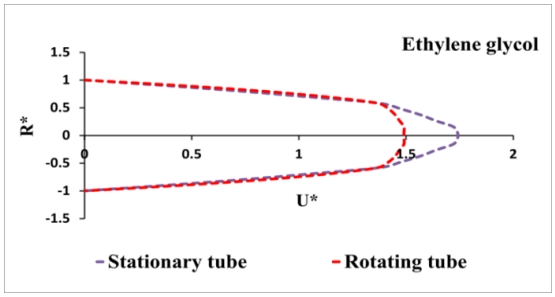

Fig.6(C) The predicted dimensionless axial velocity (U*) profiles on cross-sectional planes, at position, X* = 0.85 from tube inlet, for Ethylene glycol in the stationary and rotating tubes, at u_i = 0.6 m/s, n = 1000 rpm.

Radial and tangential velocity components acting between the rotating tube wall and the fluid provide a better thermal contact between the tube wall and the fluid and hence enhance the temperature gradient, which ultimately leads to a high heat transfer rate.

The dimensionless radial and tangential velocity profiles are plotted at different axial positions from tube inlet, as illustrated below.

Figures 7 and 8 illustrate the radial velocity component contours (v) and the predicted dimensionless radial velocity component profiles, respectively, for all fluids inside the stationary and rotating tubes. As seen in these figures, the change in the radial velocity component due to the rotation is not large, especially in the tubes with Engine oil and Ethylene glycol. According to that, its effect on enhancement of the heat transfer will ignore.

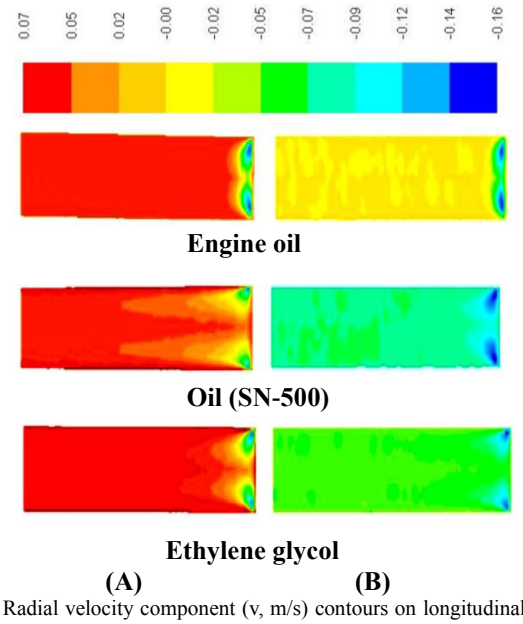

Fig.7 Radial velocity component (v, m/s) contours on longitudinal planes, from tube inlet to X* = 0.15, for all fluids in the stationary and rotating tubes, at u_i = 0 .6 m/s, n = 1000 rpm. (A): Stationary tubes, (B): Rotating tubes.

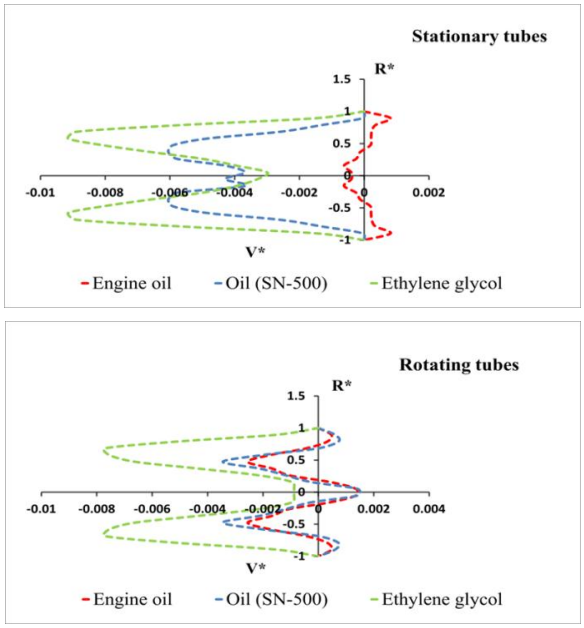

Fig.8 The predicted dimensionless radial velocity (V*) profiles on cross-sectional planes, at position, X* = 0.08 from tube inlet, for all fluids in the stationary and rotating tubes, at u_i = 0.6 m/s, n = 1000 rpm.

Tangential velocity component in stationary tubes is nearly zero, but when the rotation is introduce into flow, it will increase toward the wall. Figures 9 and 10 represent contours of the tangential velocity component and the predicted dimensionless tangential velocity component profiles in the rotating tubes. It is seen that the tangential velocity component in the tube with Ethylene glycol is more affected by rotation than that for the tubes with Engine oil and Oil (SN-500). It is fact that the effect of rotation is increased with decreasing of viscosity of the working fluid**.**

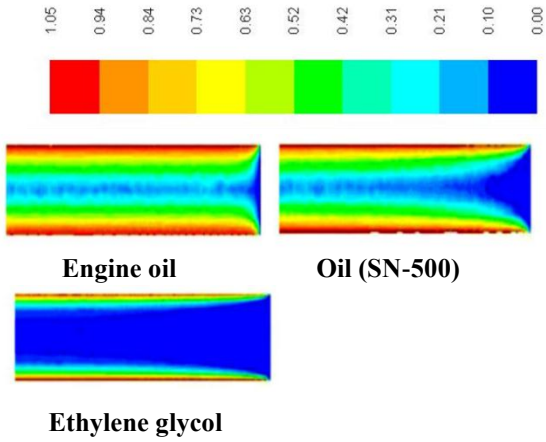

Fig.9 Tangential velocity component (w, m/s) contours on longitudinal planes, from tube inlet to X* = 0.15, for all fluids in the rotating tubes, at u_i = 0.6 m/s, n = 1000 rpm.

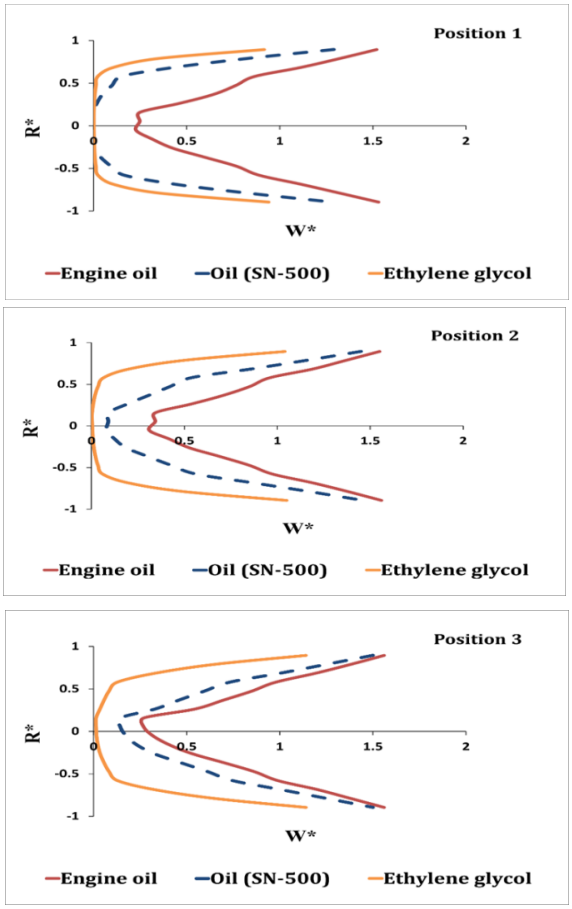

Fig.10 The predicted dimensionless tangential velocity (W*) profiles on cross-sectional planes, at positions 2 and 3, which equal to X* =0.01, 0.05 and 0.08 from tube inlet, respectively, for all fluids in the rotating tubes, at u_i = 0.6 m/s, n = 1000 rpm.

FRICTION FACTOR

Figures 11 and 12 explain the effect of rotation and Re on the average friction factor, for all fluids in the stationary and rotating tubes, respectively. Figs. 13 and 14 illustrate the change of the average friction factor ratio with Re_ω and Re, respectively. These figures show that, for all Re considered, the average value of the friction factor increases with the increase in the rotation Reynolds number, as shown in Figs. 11 and 12. This is due to the stabilizing effect induced by rotation on the flow, which becomes more remarkable when the rotation speed increases. The results also show that, at higher rotation Reynolds number (i.e., n = 500, 1000 and 2000 rpm), the tubes with Ethylene glycol give higher friction factor ratio than that for the tubes with Engine oil and Oil (SN-500) (Figs. 13 and 14). This is because the higher rotation speed reduces the developing length, which results in decrement the fluid velocity along tube (see Figs.5 and 6(A, B, and C)). Generally, friction factor increased by rotation to about 15-193 % in the tubes with Engine oil, 13-125 % in the tubes with Oil (SN-500) and 12-619 % in the tubes with Ethylene glycol.

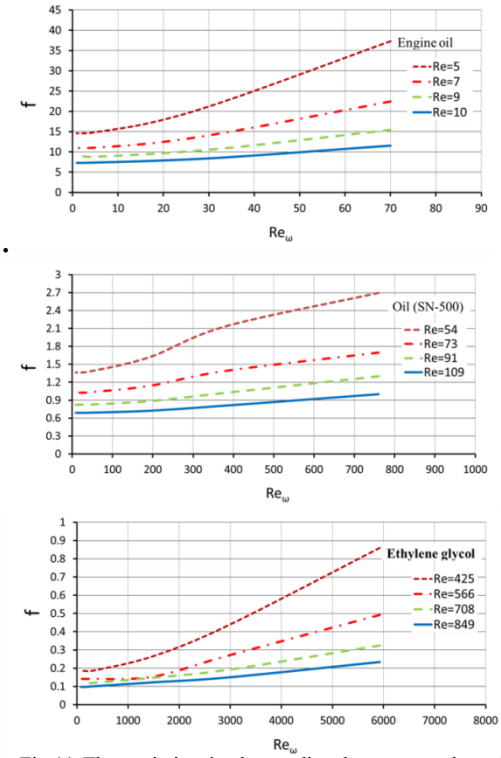

Fig.11 The variation in the predicted average value of the friction factor with rotation Reynolds number, for all fluids, at different Reynolds numbers.

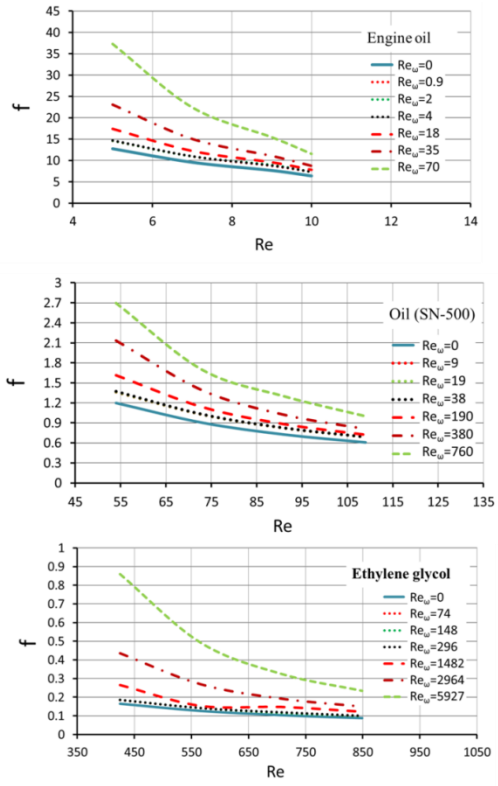

Fig.12 The variation in the predicted average value of the friction factor with Reynolds number, for all fluids in the stationary and rotating tubes, at different rotation Reynolds numbers.

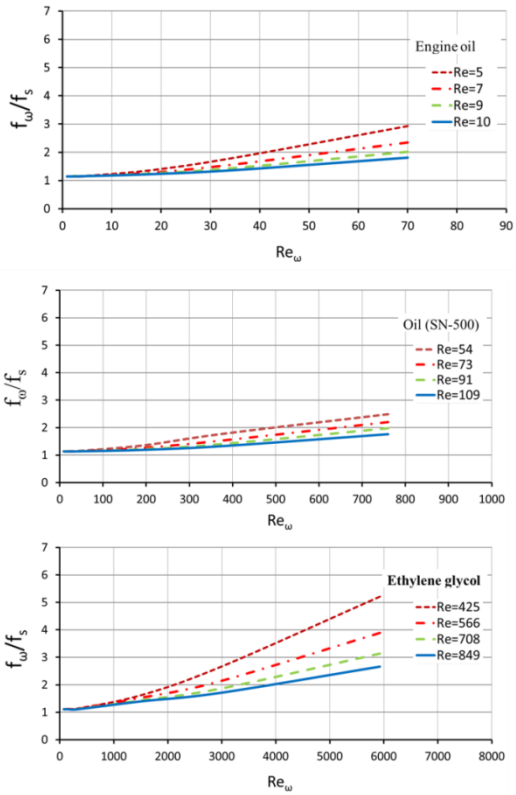

Fig.13 The variation in the predicted average value of the friction factor ratio with rotation Reynolds number, for all fluids.

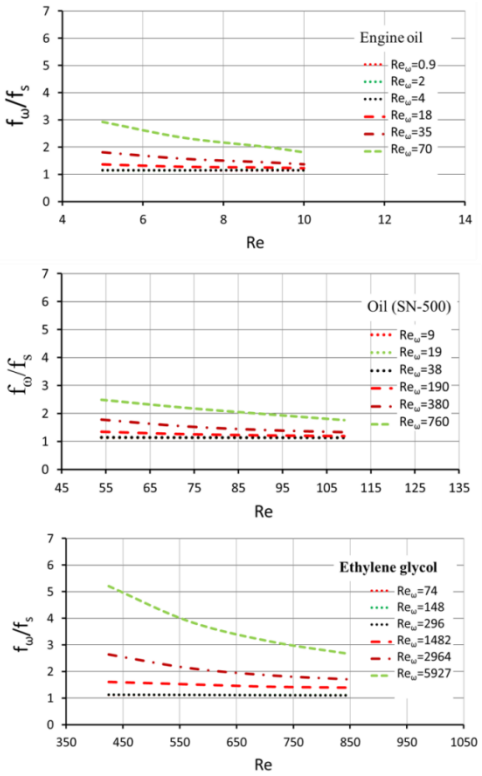

Fig.14 The variation in the predicted average value of the friction factor ratio with Reynolds number, for all fluids.

6.2 THERMAL FIELD INVESTIGATIONS

In this study, enhancement of the heat transfer is depended on the tangential velocity component, which enhances the heat transfer across fluid layers. Therefore, the average Nu in the rotating tubes is expected to be higher than that observed in the stationary tubes.

Figures 15 and 16(A and B) depict the predicted temperature contours and the dimensionless temperature profiles, respectively, for all fluids inside stationary and rotating tubes. It's seen that rotation improves the temperature gradients near the tube wall than those for case without rotation, which leads to enhancement the rate of heat transfer.

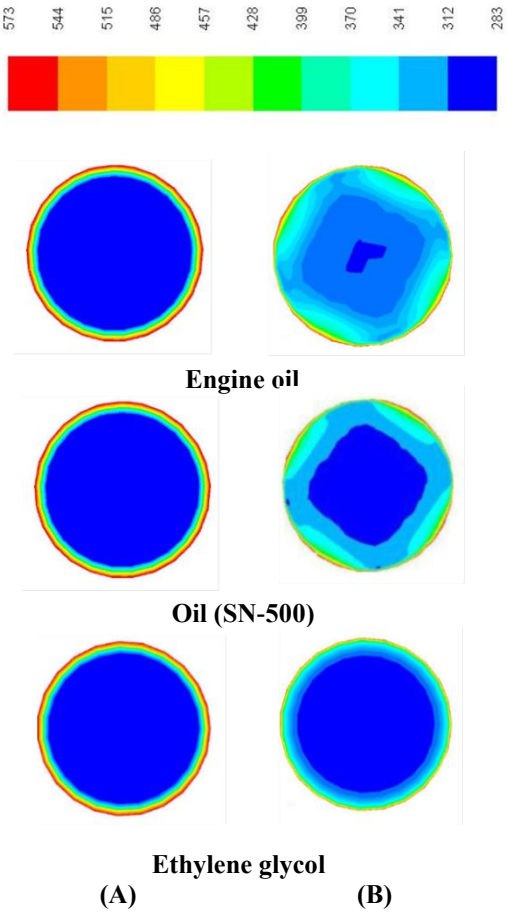

Fig.15 The predicted temperature,T (K) contours on cross-sectional planes, at X* = 0.9 from tube inlet, for all fluids in the stationary and rotating tubes, at u_i = 0.6 m/s, n = 1000 rpm. (A): Stationary tubes, (B): Rotating tubes.

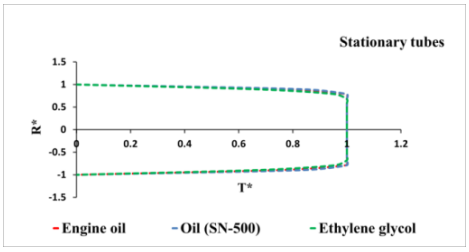

Fig.16(A) The predicted dimensionless temperature (T*) profiles on cross-sectional planes, at position, X* = 0.9 from tube inlet, for all fluids in the stationary tubes, at u_i = 0.6 m/s, n = 1000 rpm.

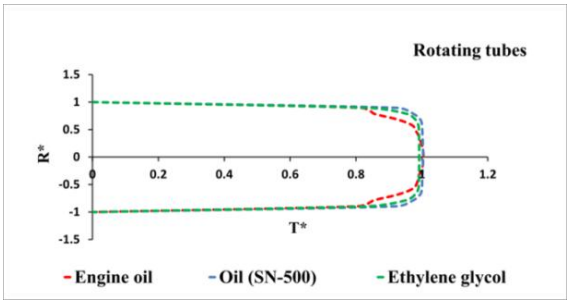

Fig.16(B) The predicted dimensionless temperature (T*) profiles on cross-sectional planes, at position, X* = 0.9 from tube inlet, for all fluids in the rotating tubes, at u_i = 0.6 m/s, n = 1000 rpm.

HEAT TRANSFER

Figures 17 and 18 illustrate the effect of the rotation and Reynolds number on the average value of Nu, respectively. From Fig. 17, it is found that, at each Re considered, the average Nu of the fluids increases as the Re_ω. This is because of the increase in the tangential velocity component as rotation speed increases.

From Fig. 18, it is seen that, average Nu of the fluids in rotating tubes slightly increases with Re. This is attributed to the rotation effect on the flow which increases as the Re increases, where improvement of the tangential velocity component by rotation reduces when the Re increases.

Variation of the Nu ratio with the Re_ω and Re are illustrated in the Figs. 19 and 20, respectively. These figures indicate that, at higher Re_ω (with n = 500, 1000 and 2000 rpm), the tubes with Ethylene glycol yield low enhancement ratio of the heat transfer than that for the tubes with Engine oil and Oil (SN-500). It is because of the viscous effects which significantly increased in the flow when rotation speed increased. These effects weaken growing of the tangential velocity component at the tube center and causes small temperature gradient near the tube wall (see Figs. 10 and 16(A and B)). In addition, the heat transfer enhancement ratio in tubes with Engine oil and Oil (SN-500) decreases with the increase in Re, as a result of rotation effect on the flow. While for tubes with Ethylene glycol, this effect becomes more pronounced at the large rotation speeds due to its higher flow rate.

.At lower Re_ω (i.e. n = 25, 50 and 100 rpm), the tubes with Engine oil and Oil (SN-500) produced lower Nusselt number ratio than that for the tubes with Ethylene glycol, as shown in Figs. 19 and 20, due to the high thermal resistance of the Engine oil and Oil (SN-500). However, Nu increases by rotation to about 24-309 % in the tubes with Engine oil, 0.85-206 % in the tubes with Oil (SN-500) and 30-133 % in the tubes with Ethylene glycol.

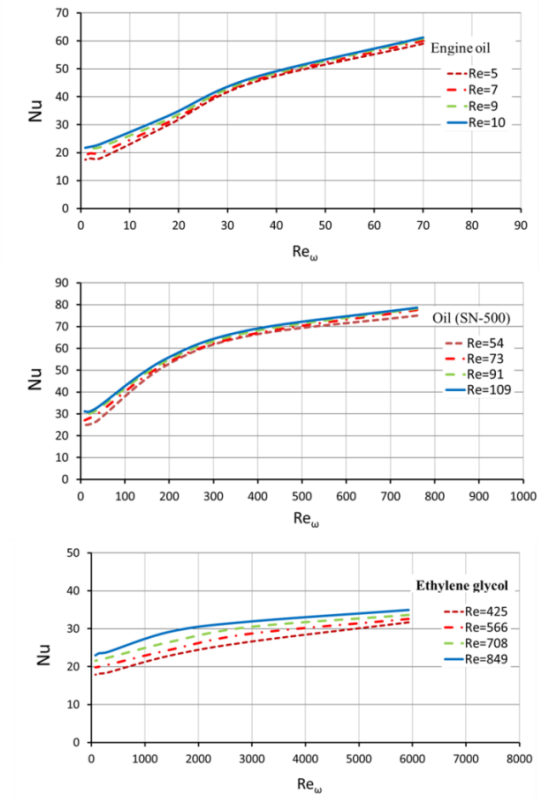

Fig.17 The variation in the predicted average value of the Nu with Re_ω , for all fluids, at different Re.

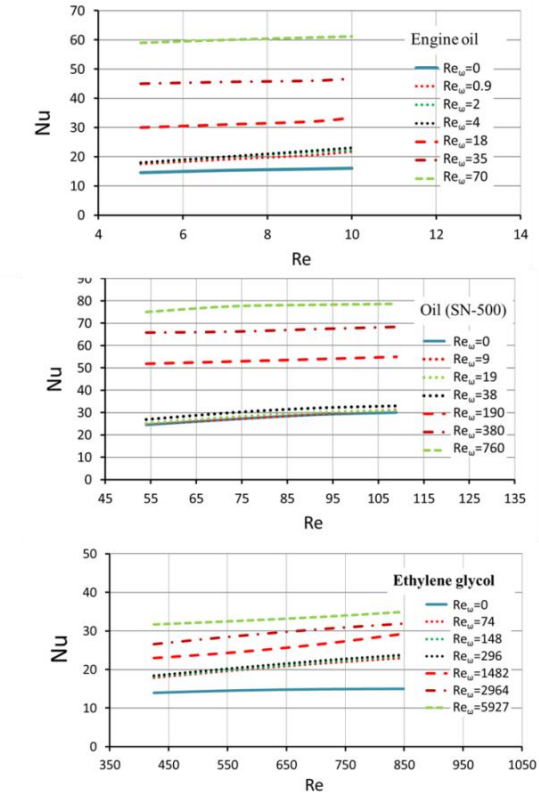

Fig.18 The variation in the predicted average value of the Nu with Re, for all fluids in the stationary and rotating tubes, at different Re_ω.

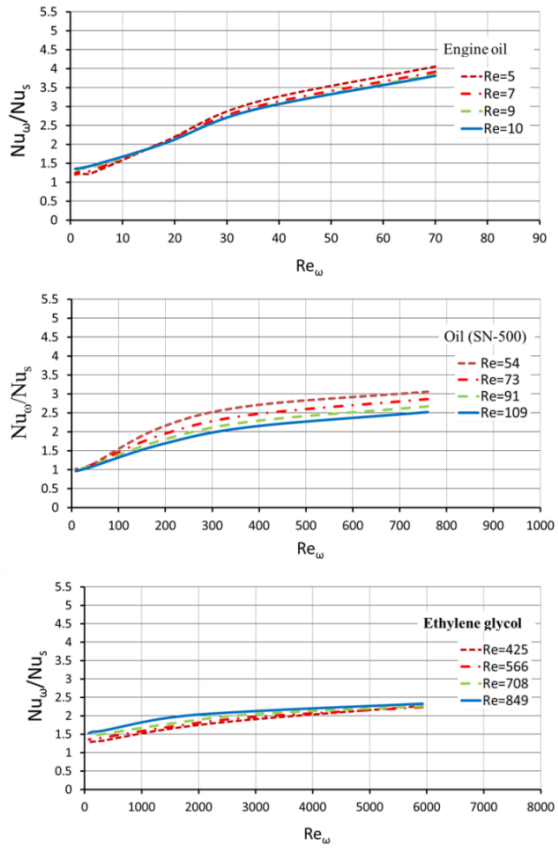

Fig.19 The variation in the predicted average value of the Nu enhancement ratio with Re_ω for all fluids..

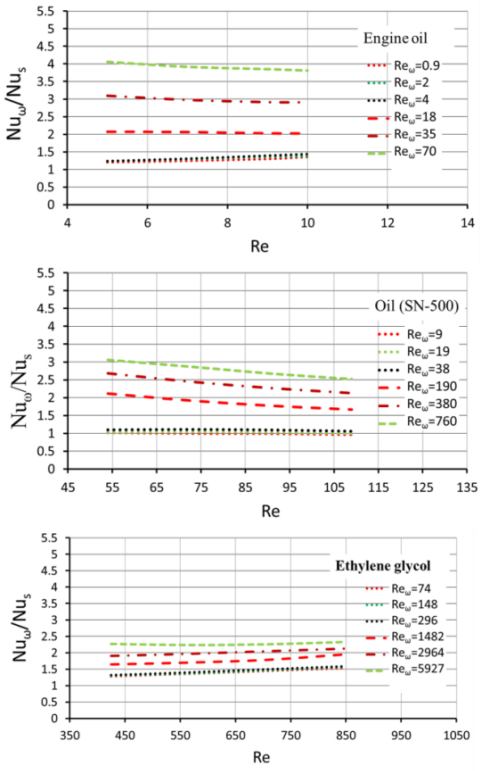

Fig.20 The variation in the predicted average value of the Nu enhancement ratio with Re for all fluids.

6.3 THERMAL PERFORMANCE FACTOR

Figures 21 and 22 give the variation of the thermal performance factor (TPF) with the Re_ω and Re, respectively, for all fluids inside rotating tubes. It is clearly seen from Fig. 21 that the thermal performance factor for tubes with Ethylene glycol is more affected by rotation speed, where it reaches the maximum values at $Re_\omega = 296$ (with n = 100 rpm), then go down as rotation speed increases. In the tubes with Engine oil and Oil (SN-500), the TPF reaches its maximum values at $Re_\omega = 35$ and 380 (n = 1000 rpm) respectively, then decreases with increase of the Re_ω.

Maximum values of the thermal performance are obtained at higher Re, as shown in Fig.22, which are about 2.1, 1.6 and 1.44 at Re = 11, 109 and 849 for the tube with Engine oil, Oil (SN-500) and Ethylene glycol, respectively.

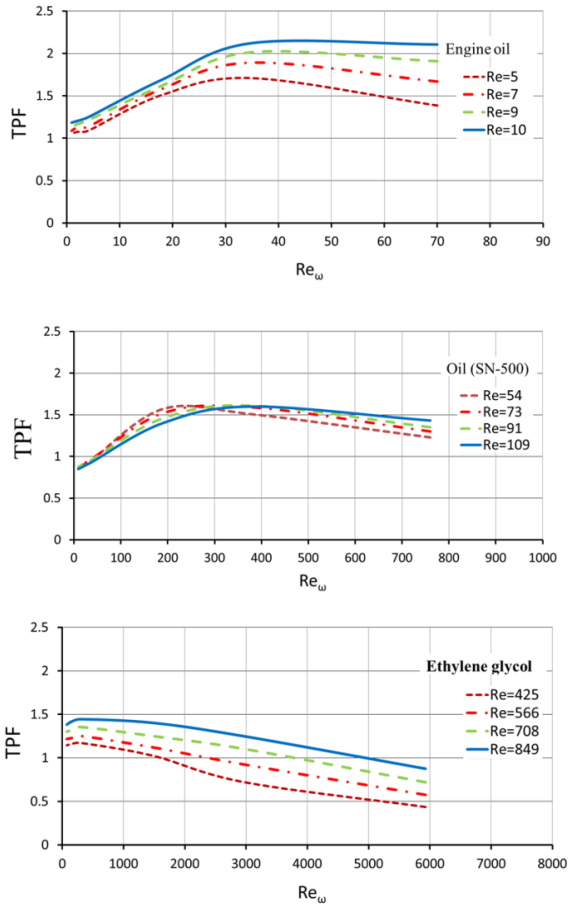

Fig.21 The variation in the thermal performance factor with Re_ω for different fluids.

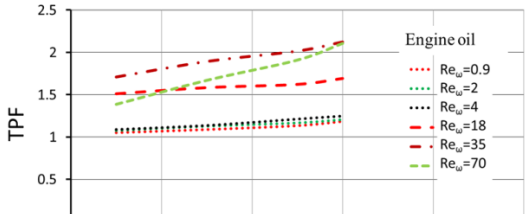

Fig.22 The variation in the TPF with Re for different fluids.

CONCLUSIONS

Fluid flow and heat transfer characteristics for three different high viscous fluids on laminar flow inside axially rotating tubes with constant surface temperature have been investigated numerically using ANSYS FLUENT 14.0. The computational results show that, when the rotation is introduced into the flow by rotating the tube about its axis, no change in flow pattern of fluids was noticed and the flow of the fluids along the rotating tubes was more stable than the flow along the stationary tubes. Therefore, in this study, the enhancement of heat transfer by rotation is due to the tangential velocity component and the thermal effects of the fluids on the heat transfer. In tubes with Ethylene glycol, the increase in the rotation Reynolds number resulted in increase the viscous effects in the boundary layer than those in tubes with Engine oil and Oil (SN-500). This leads to decrease the enhancement of heat transfer at the wall, as compared with the tubes with Engine oil and Oil (SN-500). In general, in tubes with Ethylene glycol, the friction factor is more sensitive to the tube rotation than the heat transfer; therefore, the high rotation speed (i.e. n = 500, 1000 and 2000 rpm) is unfavorable to enhance the thermal performance for the tubes with Ethylene glycol. Contrarily, in the tubes with Engine oil and Oil (SN-500), the thermal performance can enhance in cases with a suitable rotation speed (n = 1000 rpm).

NOMENCLATURE

A_s	Surface area, m^2
C_f	Dimensionless skin friction coefficient
C_p	Specific heat, J/kg K
D	Tube diameter, m
f	Average friction factor= $4C_f$
$\frac{f_\omega}{f_s}$	Friction factor ratio
h	Average convective heat transfer coefficient, W/m^2 K
k	Thermal conductivity, W/m.K
L	Tube length, m
$\dot{m}$	Mass flow rate of fluid, kg/s
N	Rotation rate = $\frac{W_w}{u_i}$
Nu	Average Nusselt number
$\frac{Nu_\omega}{Nu_s}$	Nusselt number ratio
n	Rotation speed, rpm
Pr	Prandtl number = $\frac{\nu}{\alpha} = \frac{C_p\mu}{k}$
p	Pressure, Pa
Q	Total rate of heat transfer, W
Re	Reynolds number = $\frac{u_i D}{\nu}$
Re_ω	Rotation Reynolds number
R_ω	Rotation number = $\frac{Re_\omega}{Re}$
T	Temperature, K
TPF	Thermal performance factor
u_i	Inlet velocity, m/s
u	Axial velocity component, m/s
v	Radial velocity component, m/s
w	Tangential velocity component, m/s
W_w	Tangential speed of the tube wall, m/s
x	Axial distance, m
x	Axial (flow) direction
X*	= x/L
U*	= u/u_i
V*	= v/u_i
W*	= w/u_i
T*	= $\frac{T_s - T}{T_s - T_i}$
x,r, z	System coordinate

GREEK SYMBOLS

α	Thermal diffusivity, m^2/s
Δ	Difference of variable
ΔT_m	logarithmic mean temperature difference, K
μ	Dynamic viscosity, kg/m.s
ν	Kinematic viscosity = $\frac{\mu}{\rho}$, m^2/s
ρ	Fluid density , kg/m^3
τ	stress tensor, N/m^2
τ_s	Wall shear stress, N/m^2
ω	Angular velocity = $\frac{2\pi n}{60}$, rad/s

SUBSCRIPTS

e	Exit
f	Fluid
i	Inlet
o	Outlet
s	Stationary
w	Wall
ω	Rotation

SUPERSCRIPTS

*	Dimensionless

REFERENCES

[1] A. White, 1964. Flow of a Fluid in an Axially Rotating Pipe, Journal of Mechanical Engineering Science, Vol. 6, No 1.

[2] Pedly, T.J, 1969. On the stability of viscous flow in a rapidly rotating pipe, J. Fluid Mech., vol. 35, No.1, pp. 97.

[3] Najib, H. M., Wolf, L., Lavan, Z. and Feger, A.A, 1969. On the Stability of the Flow in Rotating Pipes, Aerospace Research Laboratories Report, No. 69-9176. P.1.

[4] K. Nishibori, K. Kikuyama, and M. Murakami, 1986. Instability of laminar boundary layer in an axially rotating pipe, Fluid mechanics conference.

[5] G. Reich and H. Beer, 1989. Fluid flow and heart transfer in an axially rotating pipe—II. Effect of rotation on turbulent pipe flow, International Journal of heat and mass transfer, Vol. 32, pp. 551-562.

[6] G. Reich and H. Beer, 1989. Fluid flow and heart transfer in an axially rotating pipe—II. Effect of rotation on laminar pipe flow, International Journal of heat and mass transfer, Vol. 32, pp.563-574.

[7] Imao, S, Zhang, Q and Yamada, Y, 1989. The Laminar Flow in the developing region of a Rotating Pipe, Japan Society of Mechanical Engineers International Journal, Series II, Vol. 32, pp. 317-323.

[8] C. Y. Soong, S. T. Lin and G. J. Hwang, 1991. An Experimental Study of Convective Heat Transfer in Radially Rotating Rectangular Ducts, J. Heat Transfer, 113(3), pp. 604-611.

[9] B. Weigand and H. Beer, 1992. Fluid Flow and Heat Transfer In an Axially Rotating Pipe: The Rotational Entrance, Institute for Technical Thermodynamic, Germany.

[10] C. R. Kuo and G. J. H. wang, 1994. Aspect Ratio Effect on Convective Heat Transfer of Radially Outward Flow in Rotating Rectangular Ducts, International Journal of Rotating Machinery 1994, Vol. 1, pp. 1-18.

[11] K. C. Cheng and Liqiu Wang, 1995. Secondary Flow Phenomena in Rotating Radial Straight Pipes, International Journal of Rotating Machinery, Vol. 2, pp. 103-111.

[12] S. Torii, and W.J. Yang, 1999. Secondary Flow Phenomena in an Axially Rotating Flow Passage with sudden Expansion or Contraction. International Journal of Rotating Machinery, Vol.5, pp, 117-122.

[13] H. Chen, B. Zhang and M. Jianfeng, 2003. Theoretical and Numerical Analysis of Convective Heat Transfer in the Rotating Helical Pipes. International Journal of Heat and Mass Transfer, Vol.46, pp.4899-4909.

[14] A. O. Ojo, K. M. Odunfa, O. M. Oyewola, 2014. Numerical Simulation of the Evolution of Reynolds Number on Laminar Flow in a Rotating Pipe, American Journal of Fluid Dynamics, vol.4, pp.79-90.

[15] ANSYS FLUENT 14.0 Theory Guide. ANSYS, Inc. (2011).

[16] R.L. Webb, Performance evaluation criteria for use of enhanced heat transfer surfaces in heat exchanger design, Int. J. Heat Mass Transfer 24 (1981 715-726).

Table 1: Fluids Properties

Properties	Engine oil	Oil (SN-500)	Ethylene glycol
Density, ρ kg/m^3	889	871.13	1111.4
Specific heat capacity, Cp J/kg K	1845	4700	2415
Thermal conductivity, k W/m K	0.145	0.131	0.252
Viscosity, μ kg/m.s	1.06	0.096	0.0157
Prandtl number, Pr	13488	3444	150

Table 2: System boundary conditions

Boundaries	U	V	W	P	T
$y = y_o$ (in stationary tube), $0 \le x \le L$	0.0	0.0	0.0	$\frac{\partial p}{\partial y} = 0.0$	T_W (constant)
$y = y_o$ (in rotating tube), $0 \le x \le L$	0.0	0.0	W_W	$\frac{\partial p}{\partial y} = 0.0$	T_W (constant)
$X = 0, 0 \le y \le y_o$	u_i	0.0	0.0	$\frac{\partial p}{\partial x} = 0$	T_f
$X = L, 0 \le y \le y_o$	$\frac{\partial u}{\partial x} = 0$	0.0	0.0	$\frac{\partial p}{\partial x} = 0$	$\frac{\partial T}{\partial x} = 0$

Table 3: The dimensionless operating variables

Fluid	Re	$Re_{,\omega}$
Engine oil	5, 7, 9 and 10	0.9, 2, 4, 18, 35 and 70
Oil (SN-500)	54, 73, 91 and 109	9, 19, 38, 181, 380 and 760
Ethylene glycol	425, 566, 708 and 849	74, 148, 296, 1482, 2964 and 5927

دراسة عدديه لسلوكيات التدفق و انتقال الحرارة للموائع عالية اللزوجة المتدفقة داخل الانابيب الدوارة

الخلاصة

تناول البحث دراسة تأثير الدوران على كل من مجال تدفق المائع من حيث توزيع السرعات و معامل الاحتكاك و المجال الحراري من حيث توزيع درجات الحرارة و معدل انتقال الحرارة باستخدام ثلاثة موائع مختلفة اللزوجة (زيت المحرك، زيت (SN-500) والإثيلين جليكول) وذلك لمعرفة سلوكيات التدفق و انتقال الحرارة للموائع عالية اللزجة داخل الأنابيب المدارة.

أنجز البحث باستخدام ANSYS FLUENT 14.0 لحل المعادلات الحاكمة للتنبوء بكل من مجالات التدفق و المجالات الحرارية ومن ثم حساب معدل انتقال الحرارة ومعامل الاحتكاك. و كانت النتائج كالآتي

- أظهرت سلوكيات التدفق وانتقال الحرارة للموائع المختلفة اللزوجة داخل الأنابيب المدارة أن نسبة تحسن انتقال الحرارة في الأنابيب المزودة بالإثيلين جليكول تزداد قليلًا في سرعات الدوران العالية (500 ، 1000 و 2000 دورة في الدقيقة) ، مقارنة بتلك الملاحظة في الأنابيب المزودة بزيت المحرك وزيت (SN-500). يرجع سبب ذلك إلى التاثيرات اللزجة التي حدثت بشكل ملحوظ في الأنابيب بالإثيلين جليكول و التي عرقلت نمو مكون السرعة التماسية في التدفق وبالتالي أضعفت التحسن في انتقال الحرارة بين جزيئات المائع.
- بلغ متوسط الزيادة في عدد نسلت نتيجة الدوران إلى حوالي 4.05 مرة في الانابيب المزودة بزيت المحرك ، 3.06 مرة في الانابيب المزودة بزيت (SN-500) و 2.32 مرة في الأنابيب المزودة بالإثيلين جليكول ، مقارنة بالأنابيب الثابتة.
- بلغ متوسط الزيادة في معامل الاحتكاك نتيجة الدوران الى حوالي 2.93 مرة في الأنابيب المزودة بزيت المحرك ، 2.48 مرة في الأنابيب المزودة بزيت (SN-500) و 5.2 مرة في الأنابيب المزودة بالإثيلين جليكول ، مقارنة بالأنابيب الثابتة.
- معامل الأداء الحراري للموائع عالية اللزوجة داخل الأنابيب المدارة يزداد بزيادة عدد رينولدز. آعلى أداء حراري في الأنابيب المزودة بزيت المحرك وزيت (SN-500) حدث في سرعة الدوران 1000 دورة في الدقيقة وفي الأنابيب المزودة بالإثيلين جليكول في 100 دورة في الدقيقة.